A novel strategy for screening bioavailable quality markers of traditional Chinese medicine by integrating intestinal absorption and network pharmacology: Application to Wu Ji Bai Feng Pill

Shengnan Duan , Lei Niu , Taijun Yin , Li Li , Song Gao , Dan Yuan , Ming Hu

PII: S0944-7113(20)30057-X
DOI: https://doi.org/10.1016/j.phymed.2020.153226
Reference: PHYMED 153226

To appear in: *Phytomedicine*

Received date: 29 January 2020
Revised date: 2 April 2020
Accepted date: 6 April 2020

Please cite this article as: Shengnan Duan , Lei Niu , Taijun Yin , Li Li , Song Gao , Dan Yuan , Ming Hu , A novel strategy for screening bioavailable quality markers of traditional Chinese medicine by integrating intestinal absorption and network pharmacology: Application to Wu Ji Bai Feng Pill, *Phytomedicine* (2020), doi: https://doi.org/10.1016/j.phymed.2020.153226

Highlights

- Intestinal absorption evaluation using Caco-2 cell culture model.
- Bioavailability-enhanced network pharmacological approach for selecting markers.
- Five bioavailable markers for the quality control of WJBFP against PD.

A novel strategy for screening bioavailable quality markers of traditional Chinese medicine by integrating intestinal absorption and network pharmacology: Application to Wu Ji Bai Feng Pill

Shengnan Duan[a,b], Lei Niu[a], Taijun Yin[b], Li Li[b], Song Gao[c], Dan Yuan[a,*], Ming Hu[b,*]

[a] Department of Traditional Chinese Medicine, Shenyang Pharmaceutical University, 103 Wenhua Road, Shenyang, 110016, China

[b] Department of Pharmacological and Pharmaceutical Sciences, College of Pharmacy, University of Houston, 4849 Calhoun Road, Houston, TX 77204-5037, USA

[c] Department of Pharmaceutical and Environmental Health Sciences, Texas Southern University, 3100 Cleburne Street, Houston, TX 77004, USA

[*] Corresponding authors

Dan Yuan, Department of Traditional Chinese Medicine, Shenyang Pharmaceutical University, 103 Wenhua Road, Shenyang, 110016, China.

E-mail address: yuandan_kampo@163.com; Fax: +86 024 23986502.

Ming Hu, Department of Pharmacological and Pharmaceutical Sciences, College of Pharmacy, University of Houston, 4849 Calhoun Road, Houston, TX 77204-5037, USA.

E-mail address: mhu@uh.edu; Fax: +1 7137431884.

Abstract

Background: Major components are often used as marker compounds for quality control of traditional Chinese medicines (TCMs). However, these compounds may not necessarily bioavailable and active in *vivo*, thereby, failing to control the "quality".

Purpose: The purpose of this paper is to develop a novel strategy integrating absorption and activity deduced from network pharmacology to identify more reasonable markers for quality control of TCM formulas using Wu Ji Bai Feng Pill (WJBFP) as an example.

Study Design: Human Caucasian colon adenocarcinoma (Caco-2) cell transport studies and a bioavailability-enhanced network pharmacological approach were integrated to identify better phytochemical markers for quality control.

Methods: The absorption of multiple components in WJBFP was evaluated by a Caco-2 cell culture model. Nine databases were used to identify potential targets in the network pharmacology analysis. Cytoscape 3.7.2 was employed for the network data integration, visualization, and centrality analysis. Molecular docking was carried out to investigate the binding affinity of the identified markers to their candidate targets.

Results: The apparent permeability coefficient (Papp) and efflux ratio (ER) of 66 compounds were determined. Five hundred and two putative targets and 187 primary dysmenorrhea (PD) related targets were identified. Twenty-two candidate targets interacting with 20 potential active compounds were screened with the putative PD related targets intersection network using Degree Centrality (DC) ranking. By integrating absorption, 16 candidate targets interacting with 8 potential active compounds were identified. Besides, 53 compounds hitting candidate targets were divided into two classes according to their DC values. Then each of the two classes of DC was stratified into two groups based on the Papp for a total of four classes. Finally, five compounds belonging to Class 1 with higher DC and higher Papp, formononetin, ferulic acid, isoliquiritigenin, neocryptotanshinone and senkyunolide A, were identified as potential bioavailable phytochemical markers for the quality control of WJBFP against PD. Furthermore, molecular docking analysis validated the interplay between candidate targets and marker ingredients.

Conclusion: A novel strategy combining intestinal absorption with network pharmacology analysis was successfully established to identify bioavailable and bioactive markers for quality control of WJBFP against PD.

Keywords: absorption; Caco-2 cell culture model; network pharmacology analysis; quality control; traditional Chinese medicine; Wu Ji Bai Feng Pill

Abbreviations

ALOX5, arachidonate 5-lipoxygenase; AR, androgen receptor; Caco-2, Human Caucasian colon adenocarcinoma; COX, cyclooxygenase; CYP19A1, Cytochrome P450 Family 19 Subfamily A Member 1; DAVID, Database for Annotation, Visualization and Integrated Discovery; DC, Degree Centrality; ER, efflux ratio; ESR1, estrogen receptor 1; HBSS, hank's balanced salt solution; KEGG, Kyoto Encyclopedia of Genes and Genomes database; MMP2, matrix metalloproteinase 2; MMP9, matrix metalloproteinase 9; MRM, Multiple Reaction Monitoring; NO, nitric oxide; NOS3, endothelial nitric-oxide synthase; NSAIDs, non-steroidal anti-inflammatory drugs; OCPs, oral contraceptive pills; Papp, apparent permeability coefficient; P_{AB}, Papp from apical side to basolateral side; P_{BA}, Papp from basolateral side to apical side; PD, primary dysmenorrhea; PG, prostaglandins; PPI, protein-protein interactions; PPARG, peroxisome proliferator activated receptor gamma; PTGS2, prostaglandin G/H synthase 2; TCM, traditional Chinese medicine; TEER, transepithelial electrical resistance; TNF, Tumor Necrosis Factor; UPLC-MS/MS, Ultra High-Performance Liquid Chromatography-tandem Mass Spectroscopy; WJBFP, Wu Ji Bai Feng Pill.

1 Introduction

Traditional Chinese Medicines (TCMs) have been widely used for thousands of years in Asian countries (Park et al., 2012). It is well-known that components in TCMs are affected by multiple factors including growing areas, climate, harvest season, etc. Therefore, it is difficult to evaluate and control their holistic qualities. According to the Chinese Pharmacopoeia (Pharmacopoeia Committee of P. R., 2015), among 1203 raw herbs, the qualities of 529 herbs are controlled using a single marker (Song et al., 2013), which is the major compound in phytochemical analysis. However, it is believed that TCMs usually interact with multiple targets through multiple pathways to exert their biological efficacies. Therefore, a single marker may not be able to accurately evaluate the biological actions and therapeutic mechanisms. Thus, there is an unmet need to develop a strategy to identify markers that can be used to evaluate the bioactivity-related qualities of TCMs.

Since absorbed constituents have a better chance to perform pharmacological actions, intestinal absorption is of importance to evaluate the efficacy of TCMs, which are often orally administrated in forms of pills, powder and decoctions. Besides, multiple ingredients in a single herb or formulation may interact with each other and improve or inhibit the absorption mutually. Even the same compound in different formulas may preform different bioavailability due to the complexity of herbal medicines. Moreover, some compounds are active in *vitro* but may not be absorbed and active in *vivo*. Therefore, randomly selecting marker compounds may not reflect the in *vivo* efficacy of

TCMs. It is necessary to evaluate the intestinal absorption to identify better marker compounds.

Due to complexity, it is difficult to identify in *vivo* active compound(s) from TCMs. Pharmacognosists can isolate and pure compounds for activity evaluations. However, in TCMs, there are many components and may interact with different targets to exert a synergistic effect. Currently, network pharmacology analysis is a new approach derived from system biology, poly-pharmacology and molecular networks (Chandran et al., 2017). It could be a powerful tool to identify active ingredients of TCMs as well as their potential targets and mechanisms at the molecular and holistic levels (Liu et al., 2015).

Primary dysmenorrhea (PD) is one of the most common gynecological disorders in young women (Oladosu et al., 2018). Most symptoms of PD could be explained by the action of uterine prostaglandins (PG). Nonsteroidal anti-inflammatory drugs (NSAIDs) are the first-line options for PD. But NSAIDs are intolerable and have various adverse effects involving disorders of the liver, kidney and digestive system (Park et al., 2014). Besides, oral contraceptive pills (OCPs) were widely used for NSAIDs-resistant PD. However, about 10% women affected by PD do not respond to these treatments (Liu et al., 2013). Currently, due to the limitations of conventional treatments, herbal therapy is considered as a feasible alternative for the treatment of PD.

Wu Ji Bai Feng Pill (WJBFP), a classical gynecological TCM formula, is usually prescribed to treat dysmenorrhoeal symptoms in China (Park et al., 2014; Rowlands et

al., 2009). WJBFP were proven to be effective in reducing PG levels and have antinociceptive qualities mediated via the somatostatin pathway (Park et al., 2014). It consists of 14 botanic and 6 animal crude materials, including *Angelica sinensis* (Oliv.) Diels., *Ligusticum chuanxiong* Hort., *Paeonia lactiflora* Pal., *Rehmannia glutinosa* Libosch., *Salvia miltiorrhiza* Bge., *Glycyrrhiza uralensis* Fisch., *Astragalus membranaceus* (Fisch.) Bge. var. *mongholicus* (Bge.) Hsiao., *Panax ginseng* C. A. Mey., *Cyperus rotundus* L., *Dioscorea opposita* Thunb., *Asparagus cochinchinensis* (Lour.) Merr., *Stellaria dichotoma* L. var. *lanceolata* Bge., *Euryale ferox* Salisb., *Gallus domesticlus* Brisson, *Cervus elaphus* Linnaeus., *Ostrea gigas* Thimberg., *Trionyx sinensis* Wiegmann. and *Tenodera sinesis* Saussure. Currently, paeoniflorin was chosen as the only chemical marker according to the Chinese Pharmacopoeia (2015 Version). The rationale of using this single compound as the marker for quality control is unclear and this control may not reflect the safety and effects of WJBFP. Moreover, the responsible active compounds of WJBFP and how they perform therapeutic effects haven't been clearly elucidated until now.

In the present study, we investigated the intestinal absorption properties of WJBFP using the Caco-2 cell culture model. Then a strategy combining intestinal absorption and network pharmacology analysis was constructed to identify compounds with high permeabilities and high activity potentials as marker compounds from WJBFP.

2 Materials and methods

2.1 Chemicals and reagents

Formic acid (LC-MS grade) and Hanks' balanced salt solution (HBSS, powder) were purchased from Sigma-Aldrich (St. Louis, USA). Acetonitrile, methanol and DMSO were acquired from EMD Millipore (Darmstadt, Germany). Distilled deionized water was prepared with the Milli-Q® Integral Water Purification System (Millipore-Sigma, Darmstadt, Germany).

2.2 Herbal prescription and drug solution preparation

WJBFP (water-honeyed pills), the products of Tong Ren Tang Pharmacy Co., Ltd. (Beijing, China, Batch No. 4035466), were purchased from Guoda Pharmacy (Shenyang, China). The WJBFP extract solution was prepared according to our previously reported procedure (Duan et al., 2017). A dry residue was recovered after evaporation in vacuum at 37 ℃ and dissolved in DMSO, then diluted in HBSS solution to get different concentration drug solutions for transport experiments and cytotoxicity assay. The final concentration of DMSO in drug solutions was controlled less than 0.5% (v/v) to ensure the cell safety.

2.3 UPLC-MS/MS analysis for components quantification

LC separation was performed on the ExionLC™ UHPLC system (SCIEX, Foster City, CA, USA) with a Waters BEH C18 column (2.1 ×100 mm, 1.7 μm, Waters, Milford, MA,

USA). Mobile phases, water with 0.1% formic acid (A) and acetonitrile (B), were applied with gradient elution optimized in the previous work (Duan et al., 2017) and the flow rate was kept at 0.4 mL/min. The column temperature was 40 ℃. A SCIEX QTRAP® 5500 LC-MS/MS system (SCIEX, Foster City, CA, USA) equipped with Turbo V^{TM} source and electrospray ionization probe was used to detect permeable compounds and operated in Multiple Reaction Monitoring (MRM) mode. WJBFP extract solution (1mg/mL) was used to optimize the MRM parameters and compound dependent parameters (Table 1). Instrument dependent parameters: curtain gas = 30 psi, IonSpray voltage = +5500/-4500 V, nebulizer gas = 55 psi, heater gas = 50 psi, source temperature = 550℃, entrance potential = 10V. All data were controlled and analyzed by Analyst (Versions 1.7) from AB SCIEX.

2.4 Caco-2 cell model and transport studies

2.4.1 Cell culture and toxicity to the Caco-2 cells during transport experiment

Cell culture procedure was according to the previous study in our lab (Gao et al., 2011). The difference of transepithelial electrical resistance (TEER) values between the blank and the monolayers above 420 ohm·cm^2 was qualified for the transport study, which was monitored using an EVOM2™ Epithelial Voltohmmeter (World Precision Instruments, FL, USA).

The MTT assay was carried out to test WJBFP extract cytotoxicity against the Caco-2 cell. The extract DMSO stock solution was diluted with DMEM to the concentration at 10, 5, 2.5, 1.25, 0.625, 0.313 mg/mL. The control for cytotoxicity study was DMEM

without WJBFP. The Caco-2 cells were incubated with drug solutions and control solutions for 6h. Each group was performed in 6 replicates. The absorbance was measured at 570 nm. The percentage of cell survival was calculated by the following formula: cell viability % = (mean absorbency in test wells)/(mean absorbency in control wells) × 100%.

2.4.2 Bi-directional transport studies

The experiment protocol and calculation were described in our previous reports (Gao et al., 2011). Experiments in triplicate were performed in HBSS. Briefly, WJBFP in HBSS solution (5 mg/mL) was loaded onto the apical side (1.5 mL, for absorption transport) or basolateral side (2.6mL, for efflux transport). Five donor samples (500 µL) and five receiver samples (500 µL) were taken sequentially at 0, 0.5, 1, 2, and 4 h followed by the addition of 500 µL of fresh donor solution to the donor side or 500 µL of fresh buffer to the receiver side. After centrifugation at 15,000 rpm for 10 min, 10 µL of the supernatant was injected for UPLC–MS/MS analysis.

2.4.3 Calculation of Papp and ER

The Papp value (cm/s) was calculated from the equation

$$Papp = (dQ/dt)/(A \times Co), \quad (1)$$

where dQ/dt, the rate of drug transport (µmol/s), is obtained by linear regression analysis of amounts transported vs the time plot; A is the surface area of the cell monolayer (4.2 cm^2); Co is the initial concentration (µM) of compounds in donor chamber. In this study, permeability was calculated by peak area for relative quantitation (Du et al., 2018).

The recovery percent of each compound was calculated using the equation,

$$\text{Recovery}\% = (M_r + M_d + M_c)/M_L \times 100\% \quad (2)$$

where M_r, M_d, M_c are the amounts of the compounds recovered from the receiver side, donor side and cell monolayer at the end of the experiment, and M_L refers the amounts of compounds loading to the donor side at the beginning of the experiment. Here the amounts were calculated by peak area of each compound multiplied by the corresponding volume.

2.5 Putative targets of WJBFP and PD related therapeutic targets

Mol2 format structures and computed descriptors information of compounds were obtained from PubChem (https://pubchem.ncbi.nlm.nih.gov/). Traditional Chinese Medicine Systems Pharmacology Database and Analysis Platform (http://ibts.hkbu.edu.hk/LSP/tcmsp.php) and Swiss Targets Prediction (http://www.swisstargetprediction.ch/) were employed to collect ingredient-related targets by searching their computed descriptors or uploading mol2 structures.

The known therapeutic targets related to PD were obtained from five sources. (1) Therapeutic Target Database (https://db.idrblab.org/ttd/, last updated by NOV, 2019); (2) DrugBank database (https://www.drugbank.ca/, v5.0); (3) NCBI Gene Database (https://www.ncbi.nlm.nih.gov/gene/); (4) GeneCards human gene database (https://www.genecards.org/); (5) DisGeNET database (http://www.disgenet.org/, v6.0). “Primary dysmenorrhea” was used as the keyword and “Homo sapiens” was selected as the organism when searching targets. All the protein names were standardized into

official gene symbols (Homo sapiens) via UniProt Knowledgebase (http://www.uniprot.org/).

2.6 Network construction and analysis

Putative compound targets-PD related targets interaction network was constructed based on the protein-protein interactions (PPI) data acquired from the Cytoscape StringApp. Cytoscape platform (Version 3.7.2) was employed for network data integration, analysis, and visualization. Moreover, the topological property, degree centrality (DC) of each node in the interaction network obtained via CytoNCA were used to screen WJBFP candidate targets.

2.7 Protein-Protein Interaction networks

The PPI networks were developed and analyzed by Cytoscape StringApp (http://apps.cytoscape.org/apps/stringappe). The minimum required interaction score was set medium.

2.8 Pathway enrichment analysis

To investigate the pathways which the putative WJBFP targets involved, a pathway enrichment analysis was performed using the Database for Annotation, Visualization and Integrated Discovery database (DAVID 6.8, https://david.ncifcrf.gov/home.jsp)

based on Kyoto Encyclopedia of Genes and Genomes database (KEGG, http://www.genome.jp/kegg/, updated on October 1, 2019).

2.9 Molecular docking analysis

AutoDock Vina platform was employed to explore the binding mode and interaction between active compounds and targets (Oleg and Arthur J., 2010). The 3D structures of ligands were obtained from PubChem. Crystallographic structures of target proteins were downloaded from RCSB Protein Data Bank (www.rcsb.org). The PDBQT format coordinate files of receptors and ligands were created using AutoDockTools (ADT, ver. 1.5.6) for further analysis. The grid optimization was carried out using Autogrid program and the grid box was centered at region covering all the identified active pocket amino acid residues. The exhaustiveness was set to the value of 20 for all docking analysis. Other settings were all set as default.

Docking simulation was accomplished under AutoDock program, and nine different modes of confirmations were generated with their respective binding energy. The lowest binding energy results were considered for further post docking analysis. Docked complex of proteins and ligands and its analogues with good binding affinities were visualized in Python Molecule Viewer (PMV, ver.1.5.6), then PyMOL (ver.1.1.7) was used to analysis the binding interaction.

3 Results

3.1 Cytotoxicity test of WJBFP extract

Cytotoxicity of WJBFP extract on Caco-2 cells was determined using MTT assay. Fig. 1 showed the cell viability after incubated with different concentrations of WJBFP extracts for 6h. The results indicated that the WJBFP extract was not toxic to the Caco-2 cells within 6h at a concentration of up to 10 mg/mL. Finally, 5 mg/mL was used in the following transport studies.

3.2 Bi-directional transport of WJBFP across Caco-2 cell monolayers

In the transport studies, 66 compounds (Table 1) were detected (signal/noise >3) in the receiver side using UPLC-MS/MS. The WJBFP composition analysis chromatogram and permeation composition chromatogram in Caco-2 cell model were displayed in Fig. S1. As summarized in Table 2, the Papp and ER values of 49 compounds were successfully calculated. These constituents were classified into three groups: low group with Papp from apical to basolateral side (P_{AB}) < $2x10^{-6}$ cm/s, moderate group with P_{AB} 2-$10x10^{-6}$ cm/s and high group with P_{AB} > $10x10^{-6}$ cm/s. Twenty-three compounds displayed high P_{AB}, ranging from 10.98 to $28.15x10^{-6}$ cm/s, indicating these compounds with more than 80% fraction could be absorbed in human and considered to be highly permeable (Artursson and Karlsson, 1991). The ER values of these compounds were 0.42-1.59, suggesting a passive diffusion mechanism (Crowe and Wright, 2012). Twenty-four compounds exhibited moderate P_{AB} of 2.04-$8.53x10^{-6}$ cm/s, 21 compounds with ER <2 (0.36-1.94) and 3 compounds with ER >2 (2.37-2.87). Two compounds,

showing low P_{AB} < $2x10^{-6}$ cm/s and one compound with ER>2, were regards as poorly absorbed compounds in *vivo*. Besides, as presented in Table 2, their recovery ranged from 28.54 to 173.77 % in bidirectional transport studies, indicating metabolisms maybe involved for some compounds.

3.3 Compounds-Putative targets network and PD related therapeutic targets

Based on the chemical profile of WJBFP we previously reported (Duan et al., 2017), 502 targets related to the 173 compounds were predicted as putative targets of WJBFP (Table S1). The network was constructed by connecting chemical components and their potential targets (Fig. 2). A large number of putative targets totaling 502 were identified if we use all 173 detectable compounds (using high-resolution mass spec) from WJBFP. However, among these 173 compounds found in WJBFP, only 66 had measurable permeability. Since only bioavailable phytochemicals have a chance to become active, we further narrowed down our putative targets to 313 by using only 66 permeable compounds (Table S1). The WJBFP permeable compounds-putative targets network was performed and shown in Fig. 3. Then 187 therapeutic targets of PD were collected after removing redundant genes (Table S2).

3.4 Identification of candidate targets for WJBFP against PD

We constructed two putative target PPI networks (Fig. S2 and Fig. S3) and one PD-related target PPI network (Fig. S4) using the StringApp. Further, to explore the pharmacological mechanisms of WJBFP against PD, we intersected the two putative

target PPI networks with PD-related target PPI networks, separately. Nodes with DC values more than the median were identified as candidate targets. Twenty-two (IL6, TP53, TNF, VEGFA, ESR1, PTGS2, CASP3, IL1B, PGR, NOS3, AR, MMP9, CCL2, PPARG, CYP19A1, MMP2, HRAS, PIK3CA, ALOX5, ESR2, CYP3A4) and sixteen (PTGS2, AR, CYP19A1, PGR, ESR1, MMP2, VEGFA, TNF, PPARG, MMP9, NOS3, CASP3, TP53, IL1B, ALOX5, IL6) candidate targets were identified, respectively. The detailed typical centralities were shown in Table S3.

3.5 Identification of potential active compounds of WJBFP against PD

Candidate targets-interacted compounds network was constructed as shown in Fig. 4. 129 compounds were predicted hitting the candidate targets against PD. Twenty potential active compounds (calycosin, formononetin, rosmarinic acid, caffeic acid, ferulic acid, isoliquiritigenin, 1,2-dihydreotanshinone I, ginsenoside Rf/isomer, liquiritigenin, ononin, senkyunolide A, 2,3-didehydrotanshinone ⅡA, cryptotanshinone, danshensu, gancaonin E, gallic acid, isocryptotanshinone Ⅱ, neocryptotanshinone, rehmapicrogenin, trigonelline) were selected with DC values more than the median. Table S4 listed their detailed information and the interacted candidate targets.

3.6 Identification of bioavailable quality markers of WJBFP against PD

As presented in Fig. 5, the candidate targets-permeable compounds network was constructed. Fifty-three compounds displayed connection with 16 candidate targets.

Eight compounds (formononetin, ferulic acid, isoliquiritigenin, neocryptotanshinone, senkyunolide A, calycosin, ononin, ginsenoside Rf/isomer) were identified as potential active permeable compounds with DC values more than the median. The detailed information was provided in Table S4, including potential compounds, permeability classification, efflux ratio and interacted candidate targets.

Furthermore, we arranged the 53 permeable compounds interacting with the candidate targets into two classifications depending on whether their DC values were above the median. Then we stratified each of the two classes of DC into two groups for a total of four quadrants using 10 x 10^{-6} cm/s as a cutoff of P_{AB} value. As shown in Fig. 6, the 53 compounds were assigned into four Classes: 5 compounds belong to Class 1; 3 compounds belong to Class 2; 17 compounds belong to Class 3; 28 compounds belong to Class 4. Specifically, the five compounds in Class 1 exhibited high permeability with ER value < 2, indicating they may display high transcellular absorption in *vivo* (80-100% fraction absorbed in human) and have more chance to generate possible therapeutic effects in *vivo*. Finally, the five compounds belonging to Class 1, formononetin, ferulic acid, isoliquiritigenin, neocryptotanshinone and senkyunolide A, were identified as potential bioavailable phytochemical markers for the quality control of WJBFP against PD.

3.7 Pathway enrichment analysis

To investigate the biological functions of the integrated targets from permeable compounds-PD related targets intersection network, the pathway enrichment analysis

was performed based on the KEGG database. Totally 32 pathways were enriched with P-value < 0.05. The pathways ranking according to the P-value and their involved genes were listed in Table S5. Illustration of associations among constituents and their classification, candidate targets and involved Top 15 pathways of WJBFP were shown in Fig. 6. Constituents of Class 1 were predicted hitting nine candidate targets (PTGS2, ESR1, NOS3, MMP9, AR, MMP2, PPARG, CYP19A1, and ALOX5). And they mainly involved in Pathways in cancer, Ovarian steroidogenesis, and Tumor Necrosis Factor (TNF) signaling pathway, Estrogen signaling pathway and Steroid hormone biosynthesis.

3.8 Molecular docking analysis

The docking analysis and binding interactions between the five potential quality markers and their connected candidate targets (PTGS2, ESR1, NOS3, MMP9, AR, MMP2, PPARG, CYP19A1, and ALOX5) were carried out using Autodock Vina platform. As summarized in Table S6, the binding energies were computed to evaluate the binding affinities of the five markers with their receptors. Usually it is believed that ligands presenting low binding free energies indicate high binding affinities to their receptors.

All the marker compounds showed relatively low binding free energies with their receptors, ranging from -6.0 to -9.8 kcal/mol. Among the five ligands docking with PTGS2 (prostaglandin G/H synthase 2), isoliquiritigenin exhibited the lowest energies (-7.9 kcal/mol). The action mode of isoliquiritigenin with PTGS2 was shown in Fig. 7a, the carbonyl group of isoliquiritigenin could form a hydrogen bond (3.13Å) with the active

pocket amino acid residue Ser530, the phenyl group could interact with Leu352 arene-H (3.91Å). Isoliquiritigenin also displayed the lowest binding energy (-9.8 kal/mol) with AR (androgen receptor), the interplay between them was depicted in Fig. 7b. The phenolic hydroxyl group of isoliquiritigenin could form a hydrogen bond with Val47 (2.41 Å). Isoliquiritigenin exhibited the best affinity (-7.7kcal/mol) to ESR1 (estrogen receptor 1). The interplay between isoliquiritigenin and ESR1 was shown in Fig. 7c, three H-bonds were observed with Gly420 (2.8Å), Arg394 (2.3Å) and Arg394 (3.1 Å) in the binding pocket of ESR1. Additionally, formononetin performed the lowest energy (-9.2 kcal/mol) with NOS3 (endothelial nitric oxide synthase). As shown in Fig. 7d, in the binding pocket of NOS3, Tyr475 form a hydrogen bond (2.1Å) with formononetin. Formononetin also showed the best affinity (-7.6 kcal/mol) to CYP19A1 (Cytochrome P450 Family 19 Subfamily A Member 1). The phenolic hydroxyl group could form a hydrogen bond with Leu477 (2.2Å, Fig. 7e).

4 Discussion

Twenty-three high permeable compounds, twenty-four moderate permeable compounds and two low permeable compounds were identified from the Caco-2 permeability assay of WJBFP (Table 2). From the network pharmacology analysis based on chemical profile, 22 candidate targets interacting with 20 potential active compounds were identified (Fig. 4, Table S4). By integrating absorption properties, 16 candidate targets interacting with 8 potential active compounds were identified (Fig. 5, Table S4). Furthermore, 53 permeable compounds hitting the 16 candidate targets were assigned into four classes based on permeability evaluation and network pharmacology features. Five compounds with relatively higher Papp and DC were identified as marker compounds for the efficacy evaluation and quality control. Moreover, molecular docking validated the interplay between the markers and their candidate targets.

Caco-2 system is one of the most extensively utilized assays for intestinal permeability assessment (Press and Di Grandi, 2008). Some researchers have investigated the transport behaviors of multi-components in TCM formulas using the Caco-2 system (Dai et al., 2008; Zheng et al., 2015). In this study, the Caco-2 cell model was used to evaluate the transport properties of WJBFP, which could provide useful information for the absorption of herbal ingredients and the inspection of herbal interaction. Firstly, the cytotoxicity effect of WJBFP extract was tested on Caco-2 cells (Fig. 1). Based on the results of MTT, a non-toxic concentration (5 mg/mL) was used in the transport studies. From the transport study, 23 high permeable compounds were identified (P_{AB} value > 10.98 x 10^{-6} cm/s, ER< 2, Table 2). This result suggested that these compounds could

be well absorbed in the intestine following the passive diffusion mechanism and perform better oral bioavailability. Among them, nine compounds belonged to phthalides, eight belonged to sesquiterpenoids, three belonged to flavonoids, two belonged to tanshinones and one belonged to phenolic acids (Table 2, Fig. 3). It was found that recoveries of compounds 13, 37, 38, 42, and 58 were less than 80%, indicating these compounds probably experienced metabolism after oral administration (Lu et al., 2008; Wang et al., 2015; Wen et al., 2012; Yan et al., 2008).

From the network pharmacology analysis based on chemical profile, 20 potential active compounds were identified (Table S3). By integrating the permeable profile, eight potential bioavailable active compounds were identified (Table S3) and classified into two classes according to Papp. Then five compounds (Fig. 6) with higher Papp (>10 × 10^{-6} cm/s) were selected as the bioavailable quality markers of WJBFP. They were strongly associated with pathways in cancer, Ovarian steroidogenesis, and TNF signaling pathways via targeting PTGS2. Additionally, they also involved in Estrogen signaling pathway and Steroid hormone biosynthesis via regulating the key candidate targets, CYP191A, ESR1, NOS3, MMP2 (matrix metallopeptidase 2) and MMP9 (matrix metallopeptidase 9). Therefore, the bioavailable quality markers may display synergistic effects against PD via regulating PTGS2 expression and hormones level.

The molecular docking analysis suggested that isoliquiritigenin has the highest binding affinities to PTGS2, AR and ESR1. Published reports showed that isoliquiritigenin could

inhibit the gene expressions of PTGS2 (also known as COX-2) (Zhou and Wink, 2019), down-regulate AR (Chen et al., 2008) and transactivate the endogenous ESR1 (Maggiolini et al., 2002). Additionally, formononetin showed good binding affinities to NOS3 and CYP19A1 in the docking analysis. It was reported that formononetin could up regulate the mRNA expression of NOS3 (Wu et al., 2010). Moreover, ferulic acid, senkyunolide A and neocryptotanshinone were all reported to exert anti-Inflammatory activity via decreasing the expression of COX-2 or inducible NOS (Or et al., 2011; Sadar et al., 2016; Wu et al., 2015). Taken together, these published results corroborate our results of our molecular docking studies.

The pathophysiology of PD is due to increased and abnormal uterine activity caused by excessive uterine PGs, specifically PGE_2 and $PGF_{2\alpha}$ (Dawood, 2006). Cyclooxygenase (COX) is the rate-limiting factor in the production of PGs and many NSAIDs target COX-1 and COX-2 (Zahradnik et al., 2010). Correspondingly, all the identified bioavailable quality markers could down regulate the COX-2 expression. Furthermore, MMP2, MMP9 and ALOX5, which are also “hit” of the markers, are also involved in the synthesis of PGs during menstrual pain. Meanwhile, the identified markers have the potential to regulate hormonal level and play a similar role as OCPs against PD via targeting AR, ESR1 and CYP19A1. Therefore, the identified bioavailable quality control markers of WJBFP possibly exert synergistic therapeutic effects against PD via regulating multiple targets and pathways and could be considered as an efficient alternative in the current treatment of PD.

The present work provides a new insight to identify more reasonable markers for quality control of TCM formulas by developing a novel strategy integrating absorption and activity deduced from network pharmacology. There are some studies identified quality markers focusing on the potential activity via chemical profile-based network pharmacology analysis (Chen et al., 2018; Xiang et al., 2018). But without considering the bioavailability and activity, the screened markers for quality control probably will be useless for evaluating the therapeutic activity in *vivo*. In our previous study (Duan et al., 2019), we established an UHPLC-MS/MS method to simultaneously quantify multiple compounds in 19 batches of WJBFP products and identified chemical markers via multivariate statistical analysis. This commonly used component-based quality control allowed us to evaluate the chemical components in the products, which is usually affected by manufacturing procedure and growth area, climate, harvest season of the herbs. However, these markers may or may not related to in *vivo* activity or can or can't be absorbed easily. In other words, monitoring these chemical markers may not ensure consistent in *vivo* efficacy because bioavailability and binding with the disease targets were not considered. For example, albiflorin and salvianolic acid B, were used as chemical markers, however, the permeabilities of them were very low ($<2.35\times10^{-6}$cm/s, Table 2) and they connected with few candidate targets against PD (Fig. 5), which means they most likely have limited contribution to in *vivo* efficacy, thereby, using albiflorin and salvianolic acid B as the markers may be not appreciated. On the other hand, the permeabilities of the newly identified markers are higher ($> 14.29\times10^{-6}$cm/s, Table 2) and their binding affinity to the potential target are higher. These are the compounds that are related to in *vivo* efficacy. Therefore, consistency of these markers

will most likely have consistent in *vivo* efficacy. We expect that this platform can be used for quality control in TCM studies.

5 Conclusion

In this study, we established an innovative network pharmacology-based strategy incorporating absorption potentials as a measurement of a phytochemical's bioavailability to select phytochemical marker compounds for the quality control of TCMs against specific diseases. This platform integrates absorption and potential pharmacological effects rather than just focusing on phytochemicals analysis. For WJBFP, five compounds: formononetin, ferulic acid, isoliquiritigenin, neocryptotanshinone and senkyunolide A, are suggested to be selected as marker compounds for quality control because they are projected to impact this product's efficacy.

References

Artursson, P., Karlsson, J., 1991. Correlation between oral drug absorption in humans and apparent drug permeability coefficients in human intestinal epithelial (Caco-2) cells. Biochem. Biophys. Res. Commun. https://doi.org/10.1016/0006-291X(91)91647-U

Chandran, U., Mehendale, N., Patil, S., Chaguturu, R., Patwardhan, B., 2017. Network Pharmacology. Innov. Approaches Drug Discov. Ethnopharmacol. Syst. Biol. Holist. Target. https://doi.org/10.1016/B978-0-12-801814-9.00005-2

Chen, L., Cao, Y., Zhang, H., Lv, D., Zhao, Y., Liu, Y., Ye, G., Chai, Y., 2018. Network pharmacology-based strategy for predicting active ingredients and potential targets of Yangxinshi tablet for treating heart failure. J. Ethnopharmacol. 219, 359–368. https://doi.org/10.1016/j.jep.2017.12.011

Chen, S., Gao, J., Halicka, H.D., Traganos, F., Darzynkiewicz, Z., 2008. Down-regulation of androgen-receptor and PSA by phytochemicals. Int. J. Oncol. 32, 405–411. https://doi.org/10.3892/ijo.32.2.405

Crowe, A., Wright, C., 2012. The impact of P-glycoprotein mediated efflux on absorption of 11 sedating and less-sedating antihistamines using Caco-2 monolayers. Xenobiotica 42, 538–549. https://doi.org/10.3109/00498254.2011.643256

Dai, J.Y., Yang, J.L., Li, C., 2008. Transport and metabolism of flavonoids from Chinese herbal remedy Xiaochaihu-tang across human intestinal Caco-2 cell monolayers. Acta Pharmacol. Sin. 29, 1086–1093. https://doi.org/10.1111/j.1745-7254.2008.00850.x

Dawood, M.Y., 2006. Primary dysmenorrhea: Advances in pathogenesis and management. Obstet. Gynecol. 108, 428–441. https://doi.org/10.1097/01.AOG.0000230214.26638.0c

Du, T., Zeng, M., Chen, L., Cao, Z., Cai, H., Yang, G., 2018. Chemical and absorption signatures of Xiao Chai Hu Tang. Rapid Commun. Mass Spectrom. 32, 1107–1125. https://doi.org/10.1002/rcm.8114

Duan, S., Qi, W., Zhang, S., Huang, K., Yuan, D., 2017. Ultra high performance liquid chromatography coupled with electrospray ionization/quadrupole time-of-flight mass spectrometry for the rapid analysis of constituents in the traditional Chinese medicine formula Wu Ji Bai Feng Pill. J. Sep. Sci. 40, 3977–3986. https://doi.org/10.1002/jssc.201700438

Duan, S.N., Qi, W., Zhang, S.W., Huang, K.K., Yuan, D., 2019. Simultaneous quantification combined with multivariate statistical analysis of multiple chemical markers of Wu Ji Bai Feng Pill by UHPLC–MS/MS. J. Food Drug Anal. 27, 275–283. https://doi.org/10.1016/j.jfda.2018.10.004

Gao, S., Yang, Z., Yin, T., You, M., Hu, M., 2011. Validated LC-MS/MS method for the determination of maackiain and its sulfate and glucuronide in blood: Application to pharmacokinetic and disposition studies. J. Pharm. Biomed. Anal. 55, 288–293. https://doi.org/10.1016/j.jpba.2011.01.015

Liu, C., Liu, R., Fan, H., Xiao, X., Chen, X., Xu, H., Lin, Y., 2015. Network Pharmacology Bridges Traditional Application and Modern Development of

Traditional Chinese Medicine. Chinese Herb. Med. 7, 3–17. https://doi.org/10.1016/s1674-6384(15)60014-4

Liu, P., Duan, J., Wang, P., Qian, D., Guo, J., Shang, E., Su, S., Tang, Y., Tang, Z., 2013. Biomarkers of primary dysmenorrhea and herbal formula intervention: An exploratory metabonomics study of blood plasma and urine. Mol. Biosyst. 9, 77–87. https://doi.org/10.1039/c2mb25238d

Lu, T., Yang, J., Gao, X., Chen, P., Du, F., Sun, Y., Wang, F., Xu, F., Shang, H., Huang, Y., Wang, Y., Wan, R., Liu, C., Zhang, B., Li, C., 2008. Plasma and urinary tanshinol from Salvia miltiorrhiza (Danshen) can be used as pharmacokinetic markers for cardiotonic pills, a cardiovascular herbal medicine. Drug Metab. Dispos. 36, 1578–1586. https://doi.org/10.1124/dmd.108.021592

Maggiolini, M., Statti, G., Vivacqua, A., Gabriele, S., Rago, V., Loizzo, M., Menichini, F., Amdò, S., 2002. Estrogenic and antiproliferative activities of isoliquiritigenin in MCF7 breast cancer cells. J. Steroid Biochem. Mol. Biol. 82, 315–322. https://doi.org/10.1016/S0960-0760(02)00230-3

Oladosu, F.A., Tu, F.F., Hellman, K.M., 2018. Nonsteroidal antiinflammatory drug resistance in dysmenorrhea: epidemiology, causes, and treatment. Am. J. Obstet. Gynecol. 218, 390–400. https://doi.org/10.1016/j.ajog.2017.08.108

Oleg, T., Arthur J., O., 2010. AutoDock Vina: Improving the Speed and Accuracy of Docking with a New Scoring Function, Efficient Optimization, and Multithreading. J. Comput. Chem. 31, 455–461. https://doi.org/10.1002/jcc

Or, T.C.T., Yang, C.L.H., Law, A.H.Y., Li, J.C.B., Lau, A.S.Y., 2011. Isolation and identification of anti-inflammatory constituents from Ligusticum chuanxiong and their underlying mechanisms of action on microglia. Neuropharmacology 60, 823–831. https://doi.org/10.1016/j.neuropharm.2010.12.002

Park, H.L., Lee, H.S., Shin, B.C., Liu, J.P., Shang, Q., Yamashita, H., Lim, B., 2012. Traditional medicine in China, Korea, and Japan: A brief introduction and comparison. Evidence-based Complement. Altern. Med. 2012, 429103. https://doi.org/10.1155/2012/429103

Park, K.S., Park, K.I., Hwang, D.S., Lee, J.M., Jang, J.B., Lee, C.H., 2014. A review of in vitro and in vivo studies on the efficacy of herbal medicines for primary dysmenorrhea. Evidence-based Complement. Altern. Med. 2014, 296860. https://doi.org/10.1155/2014/296860

Pharmacopoeia Committee of P. R., 2015. Pharmacopoeia of People's Republic of China. China Medical Science and Technology Press., Beijing.

Press, B., Di Grandi, D., 2008. Permeability for Intestinal Absorption: Caco-2 Assay and Related Issues. Curr. Drug Metab. 9, 893–900. https://doi.org/10.2174/138920008786485119

Rowlands, D.K., Cui, Y.G., Wong, H.Y., Gou, Y.L., Chan, H.C., 2009. Traditional Chinese medicine Bak Foong Pills alters uterine quiescence - Possible role in alleviation of dysmenorrhoeal symptoms. Cell Biol. Int. 33, 1207–1211. https://doi.org/10.1016/j.cellbi.2009.03.003

Sadar, S.S., Vyawahare, N.S., Bodhankar, S.L., 2016. Ferulic acid ameliorates tnbs-induced ulcerative colitis through modulation of cytokines, oxidative stress, inos, cox-2, and apoptosis in laboratory rats. EXCLI J. 15, 482–499. https://doi.org/10.17179/excli2016-393

Song, X.Y., Li, Y.D., Shi, Y.P., Jin, L., Chen, J., 2013. Quality control of traditional Chinese medicines: A review. Chin. J. Nat. Med. 11, 596–607. https://doi.org/10.1016/S1875-5364(13)60069-2

Wang, Qi, Qian, Y., Wang, Qing, Yang, Y. fang, Ji, S., Song, W., Qiao, X., Guo, D. an, Liang, H., Ye, M., 2015. Metabolites identification of bioactive licorice compounds in rats. J. Pharm. Biomed. Anal. 115, 515–522. https://doi.org/10.1016/j.jpba.2015.08.013

Wen, X.D., Liu, E.H., Yang, J., Li, C.Y., Gao, W., Qi, L.W., Wang, C.Z., Yuan, C.S., Li, P., 2012. Identification of metabolites of Buyang Huanwu decoction in rat urine using liquid chromatography-quadrupole time-of-flight mass spectrometry. J. Pharm. Biomed. Anal. 67–68, 114–122. https://doi.org/10.1016/j.jpba.2012.04.026

Wu, C., Zhao, W., Zhang, X., Chen, X., 2015. Neocryptotanshinone inhibits lipopolysaccharide-induced inflammation in RAW264.7 macrophages by suppression of NF-κB and iNOS signaling pathways. Acta Pharm. Sin. B 5, 323–329. https://doi.org/10.1016/j.apsb.2015.01.010

Wu, J.H., Li, Q., Wu, M.Y., Guo, D.J., Chen, H. Le, Chen, S.L., Seto, S.W., Au, A.L.S., Poon, C.C.W., Leung, G.P.H., Lee, S.M.Y., Kwan, Y.W., Chan, S.W., 2010. Formononetin, an isoflavone, relaxes rat isolated aorta through endothelium-

dependent and endothelium-independent pathways. J. Nutr. Biochem. 21, 613–620. https://doi.org/10.1016/j.jnutbio.2009.03.010

Xiang, W., Suo, T.C., Yu, H., Li, A.P., Zhang, S.Q., Wang, C.H., Zhu, Y., Li, Z., 2018. A new strategy for choosing “Q-markers” via network pharmacology, application to the quality control of a Chinese medical preparation. J. Food Drug Anal. 26, 858–868. https://doi.org/10.1016/j.jfda.2017.10.003

Yan, R., Nga, L.K., Li, S.L., Yun, K.T., Lin, G., 2008. Pharmacokinetics and metabolism of ligustilide, a major bioactive component in rhizoma chuanxiong, in the rat. Drug Metab. Dispos. 36, 400–408. https://doi.org/10.1124/dmd.107.017707

Zahradnik, H.P., Hanjalic-Beck, A., Groth, K., 2010. Nonsteroidal anti-inflammatory drugs and hormonal contraceptives for pain relief from dysmenorrhea: a review. Contraception 81, 185–196. https://doi.org/10.1016/j.contraception.2009.09.014

Zheng, M., Zhou, H., Wan, H., Chen, Y.L., He, Y., 2015. Effects of herbal drugs in Mahuang decoction and their main components on intestinal transport characteristics of Ephedra alkaloids evaluated by a Caco-2 cell monolayer model. J. Ethnopharmacol. 164, 22–29. https://doi.org/10.1016/j.jep.2015.01.043

Zhou, J.-X., Wink, M., 2019. Evidence for Anti-Inflammatory Activity of Isoliquiritigenin, 18β Glycyrrhetinic Acid, Ursolic Acid, and the Traditional Chinese Medicine Plants Glycyrrhiza glabra and Eriobotrya japonica, at the Molecular Level. Medicines 6, 55. https://doi.org/10.3390/medicines6020055

Acknowledgments

The work was supported by grants from the National Institutes of Health [GM070737, CA205633], Distinguished Professor Foundation of Liaoning Province, China [51120160], and the State Scholarship Fund of China [201808210300] form China Scholarship Council.

Conflict of interest

The authors have declared no conflict of interest.

Table legends

Table 1. Compound-dependent parameters in UPLC-MS/MS analysis.

Table 2. Bi-directional Papp, ER and recoveries of permeable compounds in transport studies.

Figure legends

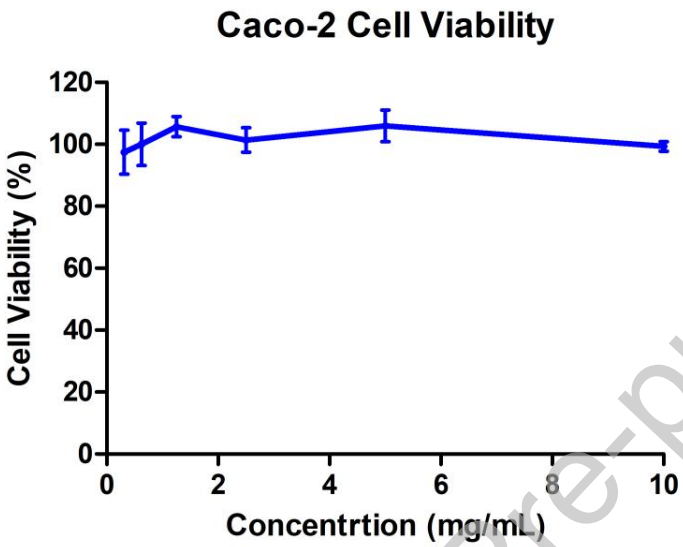

Fig.1 Effects of WJBFP extract, with different concentrations on Caco-2 cell viability using the MTT assay. Each data point represents the mean ± SD, n=6.

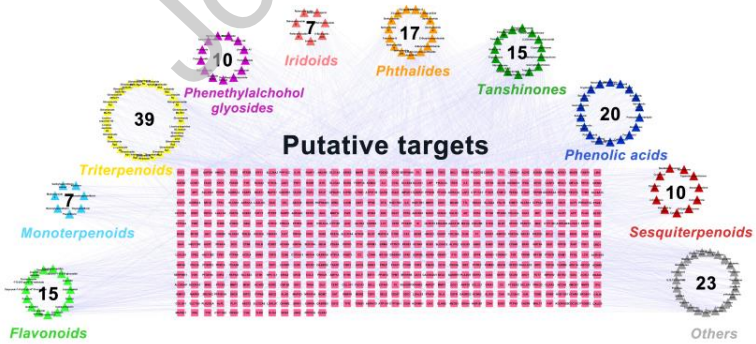

Fig. 2 Construction of WJBFP chemical compounds-putative targets network. The network was constructed by linking different types of compounds (polychrome triangles) and their putative targets (pink squares).

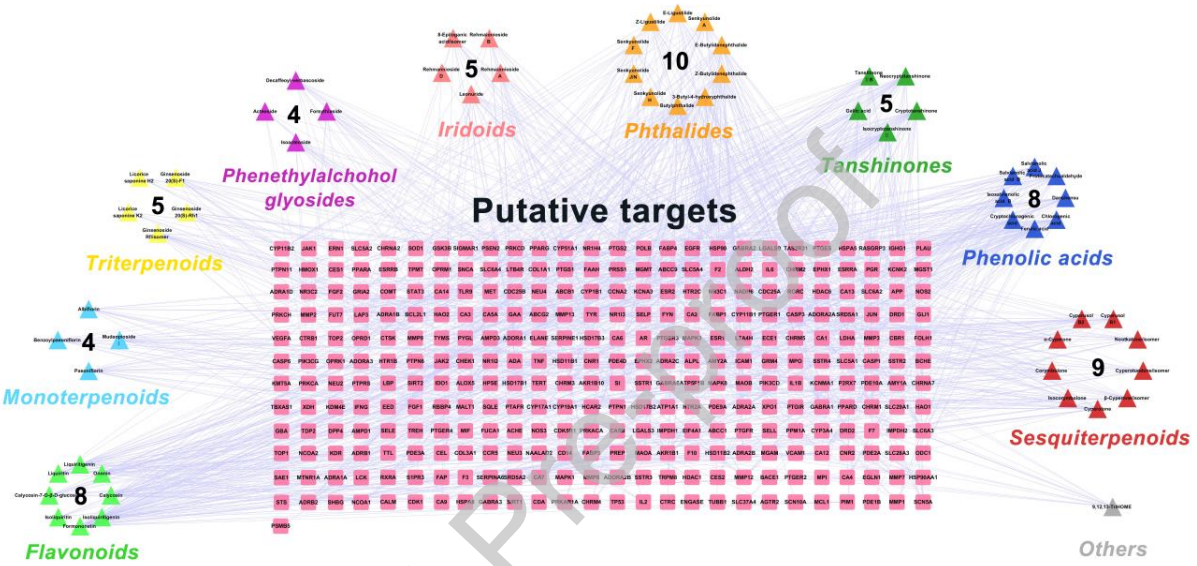

Fig. 3 Illustration of WJBFP permeable compounds-putative targets network. The network was constructed by linking the permeable compounds (polychrome triangles) and their putative targets (pink squares).

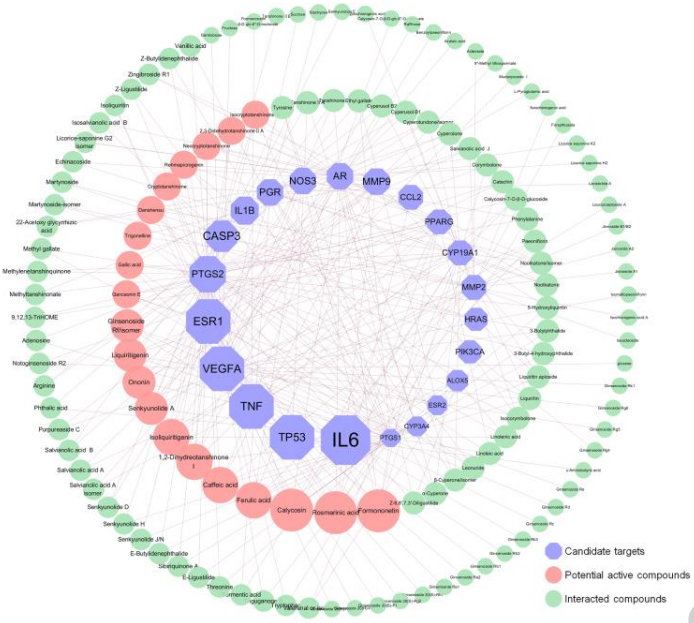

Fig. 4 Candidate targets-compounds network. Purple hexagon nodes represent candidate targets based on chemical profile networks; circle nodes represent their related compounds; pink color emphasizes the potential active compounds. The nodes size indicates the connection degree between candidate targets and compounds.

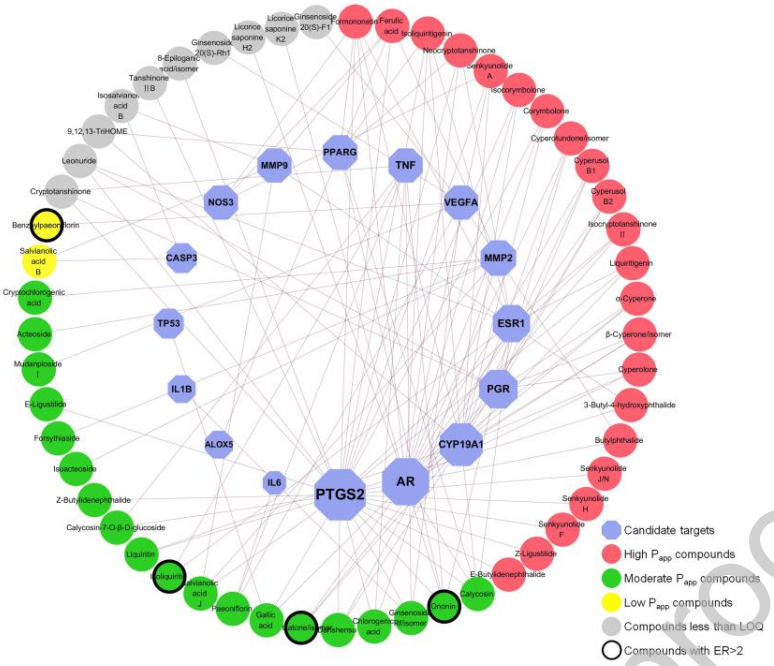

Fig. 5 Candidate targets-permeable compounds Network. Purple octagon nodes refer to candidate targets based on absorption-based networks; the circle nodes refer to interacted compounds. The red, green and yellow color refer to high, moderate and low P_{AB}; the grey nodes serve as compounds that were detectable but not quantitative. The compounds with ER above 2 were marked with black rings.

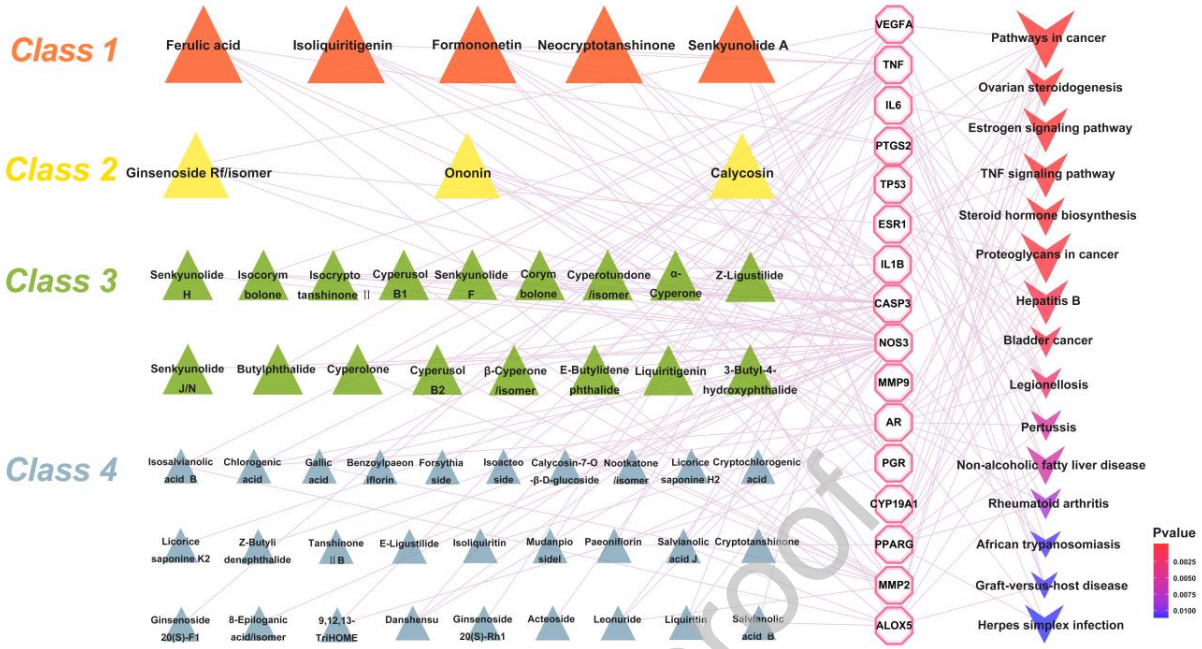

Fig. 6 Illustration of associations among classified permeable constituents, candidate targets and involved pathways. Triangles refer to permeable compounds hitting candidate targets; four different colors refer to their four quadrants classifications; octagons refer to candidate targets of WJBFP against PD; arrows refer to the enriched pathways.

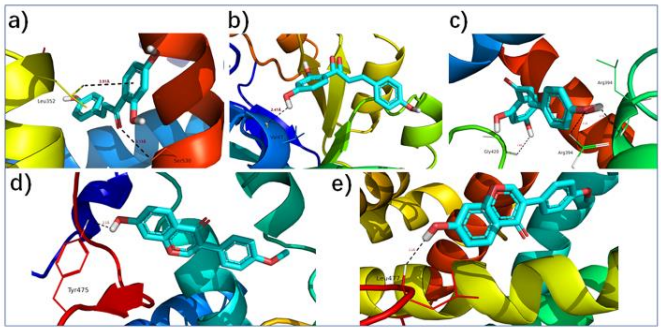

Fig. 7 Molecular docking results. The action modes of active compounds with specific proteins were calculated by Autodock Vina. a) the action mode of isoliquiritigenin and PTGS2; b) the action mode of isoliquiritigenin and AR; c) the action mode of isoliquiritigenin and ESR1; d) the action mode of formononetin and NOS3; e) the action mode of formononetin and CYP191A.

Table 1. Compound-dependent parameters in UPLC-MS/MS analysis.

No.	t_R (min)	Compounds	Q1 (*m/z*)	Q3 (*m/z*)	Dwell time (ms)	DP (V)	CE (V)	CXP (V)
1[a)]	0.72	Threonine	120.0	74.1	12.0	41.0	14.0	9.9
2[b)]	0.95	5-HMF（5-methylolfurfural）	125.0	97.0	12.0	-93.0	-21.9	-11.0
3[a)]	1.13	Tyrosine	182.1	136.1	12.0	166.0	27.0	13.3
4[a)]	1.15	Adenine	136.1	119.0	12.0	202.0	30.0	10.0
5	1.32	Gallic acid	169.0	125.0	12.0	-82.0	-20.0	-10.8
6	1.44	Rehmannioside D	685.2	179.1	12.0	-63.0	-43.0	-11.4
7[a)]	1.74	Tryptophan	205.1	188.1	12.0	296.0	15.0	11.0
8[a)]	1.76	Phenylalanine	164.1	147.1	12.0	-173.0	-18.0	-10.0
9	1.95	Danshensu	197.1	135.1	12.0	-79.0	-23.0	-15.0
10[b)]	2.20	Leonuride	393.1	167.1	12.0	-62.0	-33.0	-11.0
11[b)]	2.60	Decaffeoyl-verbascoside	461.2	179.1	12.0	-62.0	-33.0	-12.3
12[b)]	2.7	[illegible]	375.1	179.1	12.0	-68.0	-21.0	-13.2
13	2.9	[illegible]	137.0	119.0	12.0	-110.0	-26.7	-13.7
14	3.1	[illegible]	353.1	191.0	12.0	-60.0	-30.8	-12.7
15	3.56	Cryptochlorogenic acid	353.1	191.0	12.0	-60.0	-30.8	-12.7
16	4.38	Albiflorin	525.0	120.9	12.0	-47.0	-27.0	-11.0
17	4.65	Paeoniflorin	525.0	449.0	12.0	-36.0	-20.0	-13.0
18	5.07	Rehmaionioside A/B	435.1	389.1	12.0	-93.0	-18.5	-11.0
19	5.09	Ferulic acid	193.1	134.0	12.0	-56.0	-23.0	-9.0
20	5.10	Calycosin-7-O-β-D-glucoside	447.2	285.2	12.0	161.0	40.0	7.5
21	5.21	Liquiritin	417.1	255.1	12.0	-132.0	-30.0	-18.0
22	5.39	Acteoside	623.2	161.1	12.0	-104.0	-43.0	-13.0
23	5.48	Rehmaionioside A/B	435.1	389.1	12.0	-93.0	-18.5	-11.0
24	5.58	Salvianolic acid J	537.1	339.1	12.0	-78.0	-27.0	-9.0
25	5.61	Isoacteoside/Forsythiaside	623.2	161.1	12.0	-104.0	-43.0	-13.0
26	5.80	Senkyunolide J/N	227.1	209.1	12.0	121.0	20.0	16.1
27[b)]	5.86	Isosalvianolic acid B	717.1	519.1	12.0	-88.0	-27.0	-15.0
28[a)]	5.98	Azelaic acid	187.1	125.0	12.0	-60.0	-18.7	-9.0
29	6.12	Mudanpioside I	525.0	120.9	12.0	-47.0	-27.0	-11.0
30	6.29	Salvianolic acid B	717.1	519.1	12.0	-88.0	-27.0	-15.0
31	6.30	Isoliquiritin	417.1	255.1	12.0	-132.0	-30.0	-18.0
32	6.37	3-Butyl-4-hydroxyphthalide	207.1	179.1	12.0	142.0	23.8	14.0
33	6.38	Senkyunolide I	225.1	207.1	12.0	119.0	17.1	6.0
34	6.47	Ononin	431.1	269.1	12.0	90.0	41.0	19.0

Table 2. Bi-directional Papp values, efflux ratio (ER) and recoveries of permeable compounds in transport studies.

No.	Compounds name	Papp classification	P_{AB} ($\times10^{-6}$ cm/s)	P_{BA} ($\times10^{-6}$ cm/s)	ER	Recovery% (AB)	Recovery% (BA)
19	Ferulic acid	H	14.29±0.18	14.95±0.6	1.05	105.64	123.67
26	Senkyunolide J/N	H	21.15±3.28	24.24±3.52	1.15	111.64	163.19
32	3-Butyl-4-hydroxyphthalide	H	27.38±1.37	26.27±0.29	0.96	173.77	150.60
33	Senkyunolide I	H	20.67±0.2	21.9±1.31	1.06	110.57	118.12
35	Senkyunolide H	H	22.77±7.93	22.92±4.69	1.01	128.03	123.60
36	Senkyunolide F	H	25.54±2.42	21.33±1.15	0.84	118.11	131.34
37	Liquiritigenin	H	26.73±5.23	25.1±2.2	0.94	76.03	76.08
41	Neocryptotanshinone	H	16.79±0.99	19.09±1.38	1.14	157.79	130.08
42	Isoliquiritigenin	H	20.21±3.74	8.4±2.11	0.42	69.83	66.62
45	Cyperusol B1/B2 or Cyperolone	H	20.32±1.97	19.77±0.2	0.97	109.63	117.80
47	Formononetin	H	22.19±3.12	24.81±1.23	1.12	114.07	131.40
48	Corymbolone/Isocorymbolone	H	27.52±3.43	20.77±0.26	0.75	97.77	128.26
52	Cyperusol B1/B2 or Cyperolone	H	17.92±0.99	19.21±1.46	1.07	132.51	118.93
53	Senkyunolide A	H	22.05±1.04	22.31±0.57	1.01	114.80	136.88
54	Butylphthalide	H	20.14±1.04	19.86±1.22	0.99	142.57	110.96
55	Cyperusol B1/B2 or Cyperolone	H	28.15±3.62	22.19±2.3	0.79	142.25	121.29
56	Isocryptotanshinone II	H	18.2±3.88	14.67±0.3	0.81	99.07	117.12
57	Corymbolone/Isocorymbolone	H	16.79±1.87	17.98±0.15	1.07	145.58	112.47
59	E-Butylidenephthalide	H	10.98±2.61	12.48±0.75	1.14	105.92	58.58
60	Z-Ligustilide	H	14.83±3.01	26.23±1.57	1.77	105.55	86.35
62	β-Cyperone/isomer	H	16.82±0.57	18.78±1.66	1.12	91.56	94.23
63	Cyperotundone/isomer	H	19.49±2.78	20.41±3.46	1.05	128.51	80.76
66	α-Cyperone	H	18.2±1.82	28.93±4.46	1.59	105.04	79.63
5	Gallic acid	M	6.42±1.9	5.78±1.53	0.90	133.20	84.49
6	Rehmannioside D	M	2.57±0.72	4.99±1.06	1.94	107.44	91.54
9	Danshensu	M	4.71±1.49	5.99±1.74	1.27	126.27	107.80
13	Protocatechualdehyde	M	8.53±1.01	3.06±1.14	0.36	69.61	33.31
14	Chlorogenic acid	M	3.16±0.84	4.54±1.14	1.44	114.09	103.64
15	Cryptochlorogenic acid	M	3.3±1.15	4.12±0.91	1.25	121.95	131.62
16	Albiflorin	M	2.35±0.74	3.71±0.79	1.58	96.47	101.93
17	Paeoniflorin	M	5.55±1.51	8.51±1.6	1.53	129.64	106.68

Graphical abstract

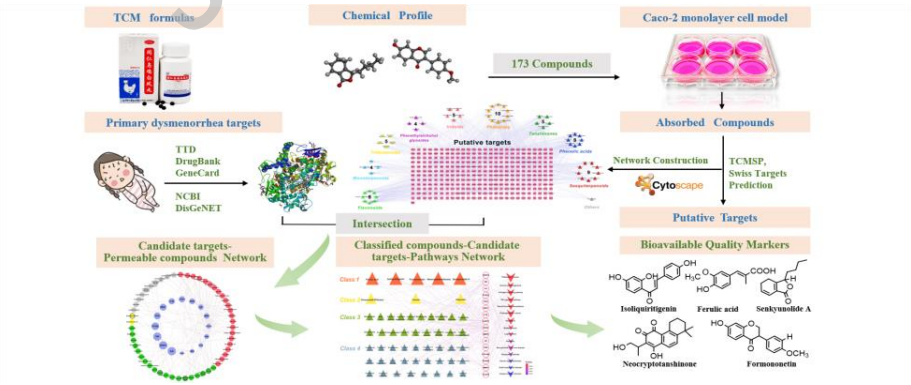

CRediT author statement

Shengnan Duan: Conceptualization, Methodology, Investigation, Writing- Original draft preparation.

Lei Niu: Data curation, Software, Formal analysis.

Taijun Yin: Resources.

Li Li: Visualization, Resources.

Song Gao: Writing- Reviewing and Editing.

Dan Yuan: Writing- Reviewing and Editing, Supervision, Funding acquisition.

Ming Hu: Writing - Review & Editing, Supervision, Project administration, Funding acquisition.